Short communication

An efficient bifunctional catalyst of TiO$_2$ coating and supported Pd on cordierite for one-pot synthesis of MIBK from acetone

Shoude Zhang, Pengcheng Wu, Lequn Yang, Yonghua Zhou *, Hong Zhong *

Chemistry and Chemical Engineering College, Central South University, Changsha 410083, China

ARTICLE INFO

ABSTRACT

We report here an efficient bifunctional catalyst of TiO$_2$ coating and supported Pd on cordierite (T500/Cor&Pd/Cor) for one-pot synthesis of MIBK from acetone. The obtained 75% MIBK selectivity at 60% acetone conversion was the best performance ever reported for metal oxide based catalyst, without obvious deactivation for at least 12 h on stream. The superior performance of T500/Cor&Pd/Cor could be attributed to the dominant base sites and moderate acid sites on TiO$_2$ coating caused by the nanoscale anatase crystallite, and its combination style of being physically mixed with Pd.

© 2015 Elsevier B.V. All rights reserved.

1. Introduction

Methyl isobutyl ketone (MIBK) has been widely used in many areas, such as paint, resins, and coating [1]. Traditionally, MIBK is mainly synthesized via a three-step process, including acid or base-catalyzed acetone condensation to diacetone alcohol (DA), acid-catalyzed dehydration of DA to mesityl oxide (MO), and metal-catalyzed hydrogenation of MO to MIBK [2]. Compared with such three-step process, one-pot synthesis of MIBK catalyzed by Pd/resin has been adopted in industry processes, which can avoid separation of the intermediates DA and MO. However, due to the high reaction pressure and low thermal stability of resin, alternative catalysts are still the research focus [3].

Supported Pd catalyst loaded on metal oxide or zeolite, such as ZSM-5 [4], SAPO [5], Al$_2$O$_3$–MgO [6], Nb$_2$O$_5$–SiO$_2$ [7], ZnO–Cr$_2$O$_3$ [8], hydroxide [9], and SiO$_2$–MgO [10] is a new type of catalyst alternative to Pd/resin catalyst over MIBK synthesis from acetone. So far, the highest acetone conversion and MIBK selectivity was reported to be Pd/Zn–Cr (1:1), having a moderate Lewis acid sites (1.2 mmol/g density), and producing MIBK with a selectivity of 78% at 40% acetone conversion [8]. In addition, HZSM-5 covered partially by SiO$_2$–ZrO$_2$ exhibited a decreased acid strength, leading to an improved acetone conversion of 33.4% and MIBK selectivity of 88.1% than that on HZSM-5 [4]. These results suggested that a satisfactory catalytic performance will be probably produced over a Pd catalyst loaded on a support with moderate acidic strength and acidic amount. TiO$_2$ has been used as solid acid and solid base for Knoevenagel [11] and aldol condensation [12]

reactions. However, TiO$_2$ is not considered for this reaction yet probably because of its low surface area unsuitable for Pd loading. Besides the effect of acid/base property of catalysts, the mass transfer limitation in pores of catalysts also plays an important role on the MIBK synthesis from acetone. Li [13] synthesized Pd-doped propyl sulfonic acid-functionalized hollow nanospheres for this reaction. These hollow nanospheres exhibited a higher activity than their bulk mesoporous counterparts, due to the short diffusion resistance of hollow nanospheres.

In this study, we deposited TiO$_2$ coating on cordierite monolith via sol–gel method and then mixed with supported Pd on cordierite, to obtain a novel physically mixed bifunctional catalyst TiO$_2$/Cor&Pd/Cor. On the one hand, we adopted physical mixing instead of loading Pd on TiO$_2$ support, trying to avoid the change of acid/base property of TiO$_2$ caused by the Pd loading process. On the other hand, TiO$_2$ coating on cordierite and Pd on cordierite ensured the completely surface distribution of both acid sites and Pd sites. As we expected, TiO$_2$/Cor&Pd/Cor presented a high activity and a high selectivity to MIBK.

2. Experimental

For the sample preparation, characterizations and catalytic tests have been shown in the experimental section in the Supporting information.

3. Results and discussion

3.1. Catalyst characterizations

The crystalline type and size of T500 powder were identified by XRD pattern (in Fig. S1) and TEM images (in Fig. 1). It was shown in Fig. S1

* Corresponding authors.
E-mail addresses: zhouyonghua@mail.csu.edu.cn (Y. Zhou), zhongh@csu.edu.cn (H. Zhong).
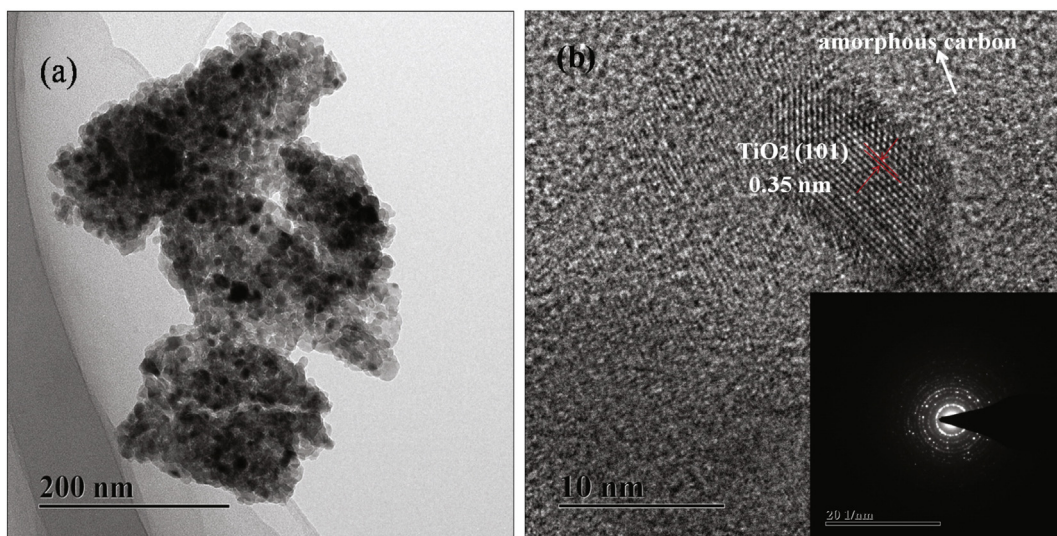
Fig. 1. TEM images of T500 powder.

that T500 was presented in the anatase phase and the crystallite size was estimated by the FWHM of characteristic peak using Scherrer's equation to be 14.1 nm (in Table S1). It was observed in Fig. 1(a) that T500 exhibited a wormhole-like mophology with small particles. The HRTEM image in Fig. 1(b) showed that TiO_2 crystallite size was about 10 nm, which was near to that estimated from XRD pattern using Scherrer's equation. In addition, carbon material was found among the TiO_2 crystallite, which was probably ascribed to the incomplete hydrolysis of tetrabutyl titanate.

The successful coating of TiO_2 on cordierite was revealed by XPS spectra and FT-IR spectra in Fig. 2. The peaks at binding energy 458.4 eV and 464.1 eV for Ti 2p could be attributed to TiO_2 [14]. The O 1s spectra were composed of two contributions. The peak at 529.5 eV for O 1s indicated that Ti ions were in an octahedral environment, which agreed with the values reported for TiO_2 [15]. In addition, a small shoulder peak at 532.1 eV denoted the presence of surface –OH groups. As for the C 1s spectra, three peaks at 284.5, 285.9, and 288.1 eV could be assigned to C–C, C–O, C═O bonds, respectively,
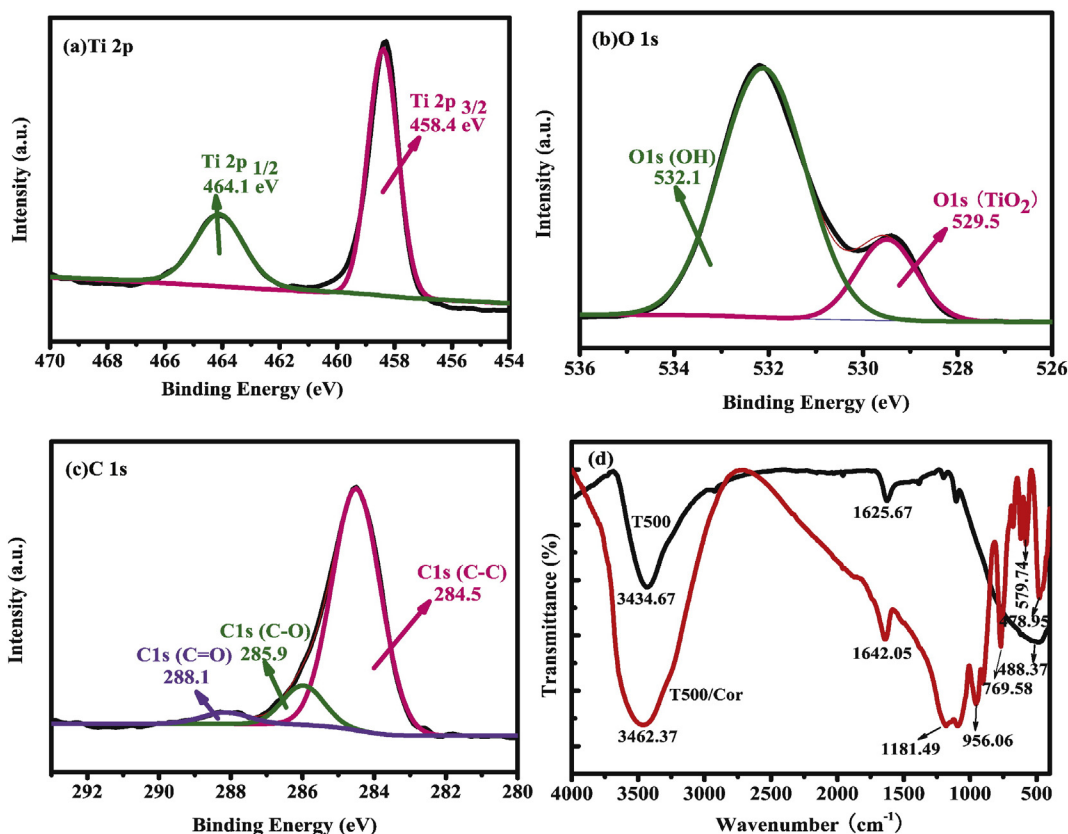

Fig. 2. XPS spectra of T500/Cor (a) Ti 2p core level, (b) O 1s core level, (c) C 1s core level, and (d) FT-IR spectra of T500 powder and T500/Cor.

indicating the incomplete hydrolysis of TiO_2 precursor [16]. Fig. 2(d) presented the FT-IR patterns of T500 powder and T500/Cor. The broad band at about 3500 cm^{-1} and the little band at 1642 cm^{-1} and 1625 cm^{-1} could be attributed to the –OH stretching vibrations and –OH bending, respectively [17]. As for T500, the broad band at 478.95 cm^{-1} reflected the Ti–O–Ti bond vibration [18]. When it was coated on cordierite, the characterization band of Ti–O–Ti network [19] was also observed indicating the presence of TiO_2 coating. Besides the two strong peaks at 1181 m^{-1} and 956 cm^{-1} were due to the Si–O–Si bending and stretching, respectively, which originated from the cordierite substrate [20].

It is difficult to evaluate the acid/base property of T500/Cor, since the surface coating is extremely thin and the content of TiO_2 coated on cordierite is determined to be 2.33 wt.% by XRF (X Ray Fluorescence) method. The NH_3-TPD and CO_2-TPD analysis results for T500 powder were shown in Fig. 3. As shown in Fig. 3(a) of NH_3-TPD, the peaks at 570 °C and 640 °C could be attributed to the moderately strong acid sites [21], and the overall amount of acid sites on T500 was calculated to be 76 μmol/g. As for CO_2-TPD profile in Fig. 3(b), two peaks were observed at 142 °C and 650 °C, respectively. The weak and moderately strong base amounts were evaluated to be 204 μmol/g and 34 μmol/g, respectively. It is indicated that TiO_2 powder is dominated by weak base sites. Meanwhile, moderate amount of strong acid sites and strong base sites presents on T500.

3.2. Catalyst tests

The representative gas-phase reaction results were shown in Table 1. When only T500/Cor was used as catalyst, the acetone conversion was 7.6% and mainly MO was produced. Some data suggested that the condensation/dehydration of acetone to MO was limited to about 20% conversion at 140 °C [22]. The value of acetone conversion is even higher than that catalyzed by MgO [10]. This means that T500/Cor has the ability to catalyze the first two steps, namely condensation and dehydration, due to the dominant base sites. We refer that the presence of large amount of base sites is greatly beneficial to the first step of acetone condensation, which is commonly regarded as the rate-controlling step in the overall one-pot process from acetone to MIBK. When Pd/Cor was mixed with T500/Cor, a much higher acetone conversion of 59.5% and MIBK selectivity of 75.2% were observed. This confirms that MO hydrogenation was readily catalyzed by Pd/Cor, which disturbs the equilibrium limitation and greatly enhances the acetone conversion. Except for MIBK, the byproducts included DIBK and C_{9+}. No intermediate product of MO was observed, indicating that the Pd/Cor amount is sufficient. In addition, it was noteworthy that no IPA was presented in all catalytic tests, which is the product of acetone hydrogenation. Research on Pd/SiO_2–ZrO_2/HZSM-5 [4] and Pd-MgO/SiO_2 [10] indicates

that the selectivity of the IPA was related to the Pd particle size. The larger the size the Pd particles are, the lesser IPA will be produced. This is probably related to the absorption model of C=O and C=C on Pd particles with different sizes [23]. As revealed by TEM result of Pd/Cor in Fig. S3, the Pd particle size ranged about 10–20 nm. In addition, it was found that the activity of T500/Cor&Pd/Cor was almost ten times higher than that of 0.7% Pd/TiO_2/Cor, although they had the same Pd loading. The bad performance of the latter could be attributed to the change of acid/base property of TiO_2 caused by Pd loading.

A series of runs at different reaction temperatures was carried out using T500/Cor&Pd/Cor bifunctional catalyst as shown in Table 1. The reaction temperature presented a significant effect on acetone conversion, increasing from 14.4% at 100 °C to 65% at 200 °C. With the increasing reaction temperature below 200 °C, a significant increase of DIBK selectivity was observed, whereas MIBK selectivity decreased monotonically. This may be explained by the enhanced formation of the over-condensation byproduct at higher reaction temperature [22]. The increase of acetone conversion suggests that the kinetics of acetone condensation also plays an important role. The acetone conversion and MIBK selectivity had slight fluctuations between 200 °C and 300 °C. When temperature was higher than 300 °C, the remarkable decline of MIBK selectivity was observed.
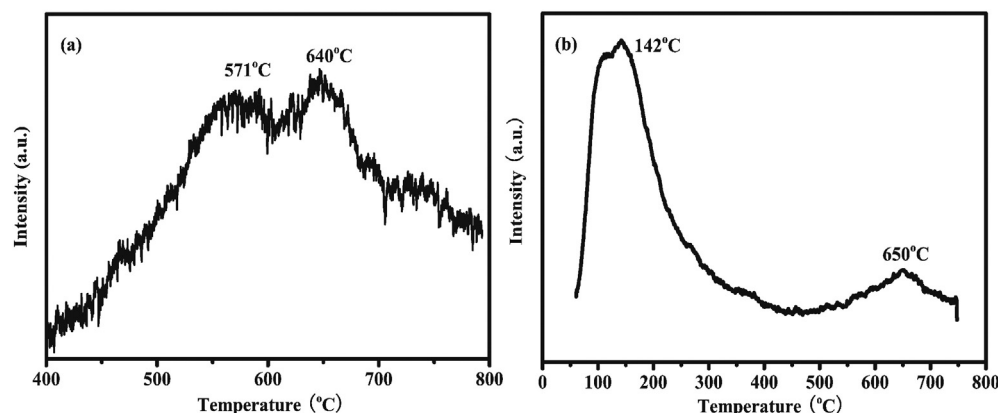
Table 1
Acetone conversion and product distribution over various catalysts.[a]

Catalyst	Conv. (%)	Selectivity (%)				
		MIBK	DIBK	Other[j]	MO	IPA
T500/Cor[d]	7.6	0.89	0	17.0	82.1	0
T500/Cor&Pd/Cor[b]	14.4	88.2	6.1	5.7	0	0
T500/Cor&Pd/Cor[c]	39.7	82.0	12.4	5.6	0	0
T500/Cor&Pd/Cor[d]	59.5	75.2	20.7	4.1	0	0
T500/Cor&Pd/Cor[e]	69.0	65.3	26.8	7.9	0	0
T500/Cor&Pd/Cor[f]	71.0	65.8	23.1	11.1	0	0
T500/Cor&Pd/Cor[g]	69.3	65.0	23.0	12.0	0	0
T500/Cor&Pd/Cor[h]	68.2	68.2	17.5	14.3	0	0
T500/Cor&Pd/Cor[i]	59.0	34.2	6.6	59.2	0	0
0.7% Pd/T500/Cor	4.8	92.9	2.6	4.5	0	0

[a] Reaction conditions: 1.5 g TX/Cor & 1.5 g Pd/Cor, 15 ml/min H_2 flow, 120 ml/min N_2 flow, GHSV = 2700 h^{-1}.
[b] Reaction temperature = 100 °C.
[c] Reaction temperature = 150 °C.
[d] Reaction temperature = 200 °C.
[e] Reaction temperature = 250 °C.
[f] Reaction temperature = 275 °C.
[g] Reaction temperature = 290 °C.
[h] Reaction temperature = 300 °C.
[i] Reaction temperature = 350 °C.
[j] Others mainly C_{9+} condensation products and mesitylene.

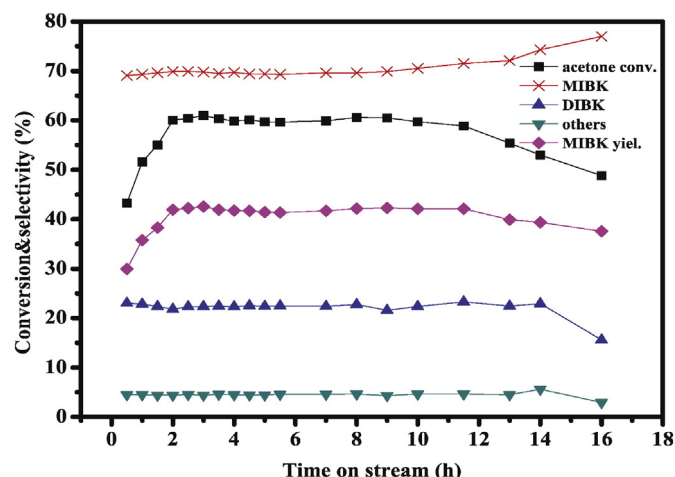**Fig. 3.** CO_2-TPD and NH_3-TPD of T500 powder.

Fig. 4. Acetone conversion and product selectivities vs. time on stream (1.5 g T500/Cor and 1.5 g Pd/Cor, 15 ml/min H$_2$ flow, 120 ml/min N$_2$ flow, GHSV = 2700 h^{-1}, 200 °C).

Besides, T500/Cor&Pd/Cor catalyst exhibited excellent stability as shown in Fig. 4. No catalyst deactivation was observed after 12 h of continuous operation at 200 °C. The catalyst reached steady state in about 2 h and after that performed with a constant 60% acetone conversion and 70% MIBK selectivity. It should be pointed out that a slow decline in acetone conversion occurred from 60% to 49% between 12 and 16 h. The stability of T500/Cor&Pd/Cor catalyst in this study overperforms those in references. So far, the best stability of catalyst was reported to be the Pd catalyst loaded on Li–Zn mixed oxides with 15 h at 120 °C [9]. The deactivation of catalyst may be due to the carbonaceous deposits, since the color of used T500/Cor becomes deeper than that of fresh catalyst.

The GSHV had no obvious effect on acetone conversion and product distribution as shown in Fig. S5. The activity and product selectivity catalyzed by T500/Cor&Pd/Cor were actually independent of the GSHV. This could be related to the complete surface distribution of acid, base and Pd sites on cordierite in this study. As we know, the TiO$_2$ coating efficiently avoids the diffusion problem that happened in porous powder catalyst. Therefore, whatever GSHV is chosen, the reactant can rapidly reach and the product can easily leave the active sites.

4. Conclusion

One-pot synthesis of MIBK from acetone is an important technology for the chemical industry. To eliminate mass transfer limitation in pores of catalysts and avoid the change of acid/base property of catalysts caused by the Pd loading process, we report a novel bifunctional catalyst composed of TiO$_2$ coating and supported Pd on cordierite monolith. TEM and XRD results revealed that T500 presented anatase crystallite with about 10 nm size. NH$_3$-TPD and CO$_2$-TPD results indicated that

T500 powder was dominated by base sites. An MIBK selectivity of 75.2% at acetone conversion of 60% was achieved using the T500/Cor&Pd/Cor at 200 °C and atmospheric pressure, and no catalyst deactivation was observed after 12 hours of continuous operation. The best run in this study gave 65% MIBK selectivity at 71% acetone conversion (46% MIBK yield) at 275 °C. The superior performance of catalyst could be attributed to the dominant base sites and moderate acid sites on TiO$_2$ coating, and its combination style of being physically mixed with Pd. Considering the facile preparation as well as the excellent catalytic performance of T500/Cor&Pd/Cor, it will be a promising alternative to the present catalysts used in MIBK synthesis from acetone.

Appendix A. Supplementary data

Supplementary data to this article can be found online at http://dx.doi.org/10.1016/j.catcom.2015.08.007.

References

[1] M.A. Alotaibi, E.F. Kozhevnikova, I.V. Kozhevnikov, J. Catal. 293 (2012) 141–144.
[2] M. Mediavilla, L. Melo, Y. Diaz, A. Albornoz, A. Llanos, J.L. Brito, Microporous Mesoporous Mater. 116 (2008) 627–632.
[3] W. Nicol, E.L. du Toit, Chem. Eng. Process. 43 (2004) 1539–1545.
[4] Y.X. Liu, K.P. Sun, X.L. Xu, X.L. Wang, Catal. Commun. 11 (2010) 322–325.
[5] S. Yang, Y.M. Wu, Appl. Catal. A 192 (2000) 211–220.
[6] Y.Z. Chen, C.M. Hwang, C.W. Liaw, Appl. Catal. A 169 (1998) 207–214.
[7] Y.Z. Chen, B.J. Liaw, H.R. Tan, K.L. Shen, Appl. Catal. A 205 (2001) 61–69.
[8] E. Kozhevnikova, I. Kozhevnikov, J. Catal. 238 (2006) 286–292.
[9] R.D. Hetterley, R. Mackey, J.T.A. Jones, Y.Z. Khimyak, A.M. Fogg, I.V. Kozhevnikov, J. Catal. 258 (2008) 250–255.
[10] J.J. Gamman, S.D. Jackson, F.A. Wigzell, Ind. Eng. Chem. Res. 49 (2010) 8439–8443.
[11] M. Pan, Y. Yang, H. Ying, X. Jia, Y. Chen, Y. Tang, Chin. J. Chem. 25 (2007) 1514–1521.
[12] J.E. Rekoske, M.A. Barteau, Ind. Eng. Chem. Res. 50 (2011) 41–51.
[13] P. Wang, S.Y. Bai, J. Zhao, P.P. Su, Q.H. Yang, C. Li, Chemsuschem 5 (2012) 2390–2396.
[14] X.Y. Xin, T. Xu, J. Yin, L. Wang, C.Y. Wang, Appl. Catal. B Environ. 176 (2015) 354–362.
[15] V.S. Mohite, M.A. Mahadik, S.S. Kumbhar, V.P. Kothavale, A.V. Moholkar, K.Y. Rajpure, C.H. Bhosale, Ceram. Int. 41 (2015) 2202–2208.
[16] M.C. Hidalgo, M. Aguilar, M. Maicu, J.A. Navio, G. Colon, Catal. Today 129 (2007) 50–58.
[17] S. Kermadi, N. Agoudjil, S. Sali, L. Zougar, M. Boumaour, L. Broch, A.E. Naciri, F. Placido, Spectrochim. Acta A 145 (2015) 145–154.
[18] X.F. Lei, X.X. Xue, H. Yang, Appl. Surf. Sci. 321 (2014) 396–403.
[19] H. Zhang, D.W. Fan, T.Z. Yu, C.L. Wang, J. Sol-Gel Sci. Technol. 66 (2013) 274–279.
[20] Y.C. Zhu, L.Y. Yu, X.F. Wang, Y.H. Zhou, H.Q. Ye, Catal. Commun. 40 (2013) 98–102.
[21] M. Watanabe, Y. Aizawa, T. Iida, R. Nishimura, H. Inomata, Appl. Catal. A 295 (2005) 150–156.
[22] A.A. Nikolopoulos, B.W.L. Jang, J.J. Spivey, Appl. Catal. A 296 (2005) 128–136.
[23] C.P. Huu, N. Keller, G. Ehret, L.J. Charbonniere, R. Ziessel, M.J. Ledoux, J. Mol. Catal. A 170 (2001) 155–163.